Heliyon 9 (2023) e13519



Contents lists available at ScienceDirect

Heliyon

journal homepage: www.cell.com/heliyon



Research article



Investigation of optical soliton solutions for the perturbed Gerdjikov-Ivanov equation with full-nonlinearity

Ismail Onder [a], Aydin Secer [b], Muslum Ozisik [a], Mustafa Bayram [b,*]

[a] Department of Mathematical Engineering, Yildiz Technical University, Istanbul, Turkey
[b] Department of Computer Engineering, Biruni University, Istanbul, Turkey

ARTICLE INFO

Keywords:
Perturbed Gerdjikov-Ivanov equation
Sardar subequation method
Modified new Kudryashov method
Optical solitons

ABSTRACT

We have discussed the perturbed Gerdjikov-Ivanov (pGI) equation describing optical pulse propagation (PP) with perturbation effects, which has various applications in optical fibers, especially in photonic crystal fibers. According to our literature review, we have discovered new and original soliton types using the Sardar sub-equation and the modified Kudryashov methods, which have not been applied to this model before. We obtained dark, bright, periodic-singular and periodic-M-shaped soliton solutions, respectively. The analytical forms of the obtained solutions are represented by 3D, 2D and contour graphics. In addition, the physical effects of the solution parameters on the wave envelope have been described and clearly interpreted by presenting their 2D graphics.

1. Introduction

Differential equations (DEs) have been used in the mathematical modeling of physical and biological phenomena for over 150 years and continue to increase in popularity rapidly. The main examples are the spread of a real disease such as Covid-19 and AIDS, shallow water waves, shock waves, energy transmission in optical fiber and magnetic media, respectively [1–4].

If the models used in the literature are examined, a large part of them consists of partial differential equations (PDEs) and nonlinear partial differential equations (NLPDEs). NLPDEs have a considerable wide usage in literature. Nonlinear Schrödinger equations (NLSEs) are one of the most widely used types of NLPDEs. NLSEs are capable of modeling large-scale media and situations due to their complex nature. Water wave modulation [5,6], application on deep water waves [7], propagation of two solitons in plasma [8], resonant waves in cold collision-less plasma media [9], solution of atomic system in chemistry [10] can be listed as some examples of variety usage of NLSEs in science. In addition, NLSEs play an important role in optic branch of physics. Optical simulation of gravity effect [11], Kerr effect [12], dark shock waves [13], chaotic behavior of NLSE system [14], solitons in thermo-optical media [15], femtosecond behavior in optical waveguide [16], stability analysis of optical solitons [17], dynamics of solitons [18], Bragg gratings [19] and much more can be cited as examples [20–23].

Moreover, in optic, there exist some phenomena equations that is based on NLSEs that describe an optical media or behavior like the optical propagation and fiber pulse propagation. Chen-Lee-Liu equation [24,25], chiral NLSE [26], Schrödinger-Hirota model [27], Kundu-Eckhaus equation [28,29], Sasa-Satsuma equation [30], $(1+1)$ dimensional perturbed NLSE [31], Biswas-Milovic equation [32,33], Ginzburg-Landau equation [34–36] and Kundu-Mukherjee-Naskar equation [37] can be briefly listed as major

* Corresponding author.
E-mail addresses: ionder@yildiz.edu.tr (I. Onder), asecer@yildiz.edu.tr (A. Secer), ozisik@yildiz.edu.tr (M. Ozisik), mustafabayram@biruni.edu.tr (M. Bayram).

https://doi.org/10.1016/j.heliyon.2023.e13519
Received 17 October 2022; Received in revised form 10 December 2022; Accepted 2 February 2023

Available online 7 February 2023
2405-8440/© 2023 The Authors. Published by Elsevier Ltd. This is an open access article under the CC BY-NC-ND license (http://creativecommons.org/licenses/by-nc-nd/4.0/).

equations. To solve our model we used the computer algebra techniques. Computer algebra is a powerful technique to solve the problem in partial differential equation [38–42].

This study examines the application of the perturbed Gerdjikov-Ivanov (pGI) equation, also known as derivative nonlinear Schrödinger-III (DNLS-III), which is based on Schrödinger equation. The pGI equation models the $(1+1)$-dimensional optical pulse propagation. The model diverges from classical Schrödinger owing to quintic nonlinearity because classical NLSE includes cubic nonlinearity.

The $(1+1)$-dimensional perturbed Gerdjikov-Ivanov equation is given as follows [43]:

$$iu_t + au_{xx} + b|u|^4u - i\left(cu^2u_x^* + du_x + \gamma\left(|u|^{2r}u\right)_x + \beta\left(|u|^{2r}\right)_x u\right) = 0, \tag{1}$$

where $u(x,t)$ is complex valued wave profile, * denotes the complex conjugate of $u(x,t)$, x is spatial and t is temporal variables, respectively. In eq. (1), the first term is linear temporal evolution, the second term is group velocity dispersion (GVD), coefficient b is the coefficient for quintic nonlinearity, d is the coefficient for intermodal dispersion, γ is the coefficient of the self-steepening term for short pulses and β, c are the coefficients of the nonlinear dispersion and lastly, r has an effect for full nonlinearity. Balance between GVD and nonlinearity rises a soliton and d, γ, β arises from perturbation effects [43]. Besides, a, b, c, d, γ and β are real valued constants. If we omit the d, γ and β, eq. (1) is degenerated to Gerdjikov-Ivanov equation.

There are some recent studies in the literature on obtaining optical solitons of the pGI equation. The analytical methods used in these papers are; modified simple equation method [44], projective Riccati equation method, solitons and modulation instability [45], trial equation method [46], exp-function and Kudryashov method [47,48], modified extended direct algebraic method [49] and extended rational sin-cos and sinh-cosh method [50]. Besides all, there are some actual papers in view of fractional calculus about pGI equation such as M-fractional pGI equation [51], fractional pGI in conformable sense [52] and Riemann-Liouville fractional pGI model [53]. In addition, conservation laws for pGI with Lie symmetries [54], abundant wave solutions [55], new solitary wave solutions [56], fractional form [57], novel optical solitons [58] and computational extracting solutions [59].

In this article, we investigate the pGI equation by two efficient analytical techniques. Sardar subequation method (SSM) [24,60] and modified new Kudryashov method (mNKM) [61,62]. Organization of the paper as follows; in section 2, obtaining nonlinear ordinary differential equation (NODE), implementation of the methods is included. Section 3 includes 3D and 2D graphs of solutions and interpretation of graphs. Lastly, section 4 includes the conclusion and evaluation of the obtained results.

2. Mathematical analysis and implementations of the methods

This section includes obtaining the NODE form of the analyzed problem with the wave transform and applying the suggested methods over this form. Both proposed methods are current methods [60,63]. The SSM method includes different solutions of the Riccati equation under different constraints [60]. Although the mNKM method [63] offers few soliton solutions, it is generally an efficient method in NLEEs solution that gives quick results, is easy to implement, does not require much mathematical processing, and is effective in obtaining result-oriented ideas. Therefore, these two methods were chosen in this study.

2.1. Obtaining NODE form of pGI equation

Consider the case $r = 1$ for pGI equation in eq. (1) with the following wave transformation;

$$u(x,t) = U(\zeta)e^{i\theta}, \ \ \zeta = x - \omega t, \ \ \theta = \mu x - \lambda t + \psi_0, \tag{2}$$

where θ is the phase component, ω is the velocity of the soliton, μ is the correspondent frequency of the wave oscillation, λ is the wave number and ψ_0 is the phase constant.

Substitute eq. (2) into eq. (1), decompose the real and imaginary parts as,

$$bU^5(\zeta) + \mu(\gamma - c)U^3(\zeta) + (\lambda + \mu(d - a\mu))U(\zeta) + aU''(\zeta) = 0, \tag{3}$$

$$U'(\zeta)(d - 2a\mu + \omega) + U'(\zeta)U^2(\zeta)(c + 3\gamma + 2\beta) = 0, \tag{4}$$

where $U'(\zeta)$, $U''(\zeta)$ denote $\frac{dU}{d\zeta}$ and $\frac{d^2U}{d\zeta^2}$. From eq. (4) the following are obtained:

$$\omega = 2a\mu - d \ \text{ and } \ \beta = -\frac{c}{2} - \frac{3\gamma}{2}. \tag{5}$$

In eq. (5), if we consider the terms U'' and U^5 in eq. (3) by using the balance principle, gives $N = \frac{1}{2}$ which is the balancing term. In this case, we need to define a transformation as $U(\zeta) = \sqrt{V(\zeta)}$. So eq. (3) is degenerated to the following NODE form:

$$4bV^4(\zeta) - 4\mu(c - \gamma)V^3(\zeta) + (4\lambda + 4d\mu - 4a\mu^2)V^2(\zeta) + 2aV(\zeta)V''(\zeta) - a(V')^2 = 0. \tag{6}$$

According to eq. (6), taking into account the terms VV'' or $(V')^2$ with V^4, N is calculated as $N = 1$ which is the balancing constant.

2.2. Implementation of SSM to the pGI equation

We propose a new approach for the solution of eq. (6) in the following form:

$$V(\zeta)=\sum_{i=1}^{N}\sigma_0+\sigma_i\Phi(\zeta)^i. \tag{7}$$

If we remember that $N=1$, eq. (7) is converted into following form:

$$V(\zeta)=\sigma_0+\sigma_1\Phi(\zeta), \tag{8}$$

where σ_0 and σ_1 are determined later, $\sigma_1\neq 0$ and $\Phi(\zeta)$ satisfies the following Riccati equation:

$$(\Phi'(\zeta))^2=\alpha_1+\alpha_2\Phi(\zeta)^2+\alpha_3\Phi(\zeta)^4, \tag{9}$$

where α_1,α_2 and α_3 are real constants. The solutions of the eq. (9) are given as follows [60]:

- **Case I:** If $\alpha_2>0$ and $\alpha_1=0$,

$$\Phi_1(\zeta)=\pm\sqrt{\frac{-pq\alpha_2}{\alpha_3}}sech_{pq}(\sqrt{\alpha_2}\zeta), \tag{10}$$

$$\Phi_2(\zeta)=\pm\sqrt{\frac{pq\alpha_2}{\alpha_3}}csch_{pq}(\sqrt{\alpha_2}\zeta), \tag{11}$$

where

$$sech_{pq}=\frac{2}{pe^{(\zeta)}+qe^{(-\zeta)}},\ csch_{pq}=\frac{2}{pe^{(\zeta)}-qe^{(-\zeta)}}.$$

- **Case II:** If $\alpha_2<0,\alpha_3>0$ and $\alpha_1=0$,

$$\Phi_3(\zeta)=\pm\sqrt{\frac{-pq\alpha_2}{\alpha_3}}sec_{pq}(\sqrt{-\alpha_2}\zeta), \tag{12}$$

$$\Phi_4(\zeta)=\pm\sqrt{\frac{-pq\alpha_2}{\alpha_3}}csc_{pq}(\sqrt{-\alpha_2}\zeta), \tag{13}$$

where

$$sec_{pq}=\frac{2}{pe^{(i\zeta)}+qe^{(-i\zeta)}},\ csc_{pq}=\frac{2i}{pe^{(i\zeta)}-qe^{(-i\zeta)}},$$

and p,q are non-zero real values.

Substitution of the eq. (8) and eq. (9) into eq. (6), gives a polynomial consisting powers of the $\Phi^i(\zeta)$ $(i=0,1\ldots 4)$. Then by collecting each coefficient of $\Phi(\zeta)$ and equating them to zero, the following system of equations is acquired:

$$\begin{aligned}
&\Phi^0(\zeta):-4a\mu^2\sigma_0^2+4b\sigma_0^4-4c\mu\sigma_0^3+4g\mu\sigma_0^3-a\alpha_1\sigma_1^2+4d\mu\sigma_0^2+4\lambda\sigma_0^2=0,\\
&\Phi^1(\zeta):-8a\mu^2\sigma_0\sigma_1+16b\sigma_0^3\sigma_1-12c\mu\sigma_0^2\sigma_1+12g\mu\sigma_0^2\sigma_1+2a\alpha_2\sigma_0\sigma_1+8d\mu\sigma_0\sigma_1+8\lambda\sigma_0\sigma_1=0,\\
&\Phi^2(\zeta):-4a\mu^2\sigma_1^2+24b\sigma_0^2\sigma_1^2-12c\mu\sigma_0\sigma_1^2+12g\mu\sigma_0\sigma_1^2+a\alpha_2\sigma_1^2+4d\mu\sigma_1^2+4\lambda\sigma_1^2=0,\\
&\Phi^3(\zeta):16b\sigma_0\sigma_1^3-4c\mu\sigma_1^3+4g\mu\sigma_1^3+4a\alpha_3\sigma_0\sigma_1=0,\\
&\Phi^4(\zeta):4b\sigma_1^4+3a\alpha_3\sigma_1^2=0.
\end{aligned} \tag{14}$$

Solving the algebraic system in eq. (14) via the appropriate computer algebra software, we acquire the following solution set:

$$\mathbf{Set}_1:\left\{\begin{array}{c}\sigma_0=-\dfrac{\sigma_1^2\mu(c-g)}{2a\alpha_3},\ \alpha_2=\dfrac{-\mu^4(c-g)^4\sigma_1^4-16a^4\alpha_1\alpha_3^3}{4a^2\mu^2\alpha_3(c-g)^2\sigma_1^2},\ \sigma_1=\sigma_1,\\ b=-\dfrac{3a\alpha_3}{4\sigma_1^2},\ d=\dfrac{-5\mu^4(c-g)^4\sigma_1^4+16a\mu^2\alpha_3(c-g)^2\left(a\mu^2-\lambda\right)\sigma_1^2+16a^4\alpha_1\alpha_3^3}{16a\mu^3\alpha_3\sigma_1^2(c-g)^2}\end{array}\right\}. \tag{15}$$

Substituting the eq. (15) into the eq. (8) along with the solutions of eq. (9) which are given in from eq. (10) to eq. (13) and considering the transformation $U(\zeta)=\sqrt{V(\zeta)}$, we obtain the solutions as follows:

$$u_{1,1}(x,t)=\left(\sigma_1\sqrt{\frac{pq\alpha_2}{\alpha_3}}sech_{pq}(\sqrt{\alpha_2}(x-\omega t))\right)^{1/2}e^{i\theta}, \tag{16}$$

$$u_{1,2}(x,t)=\left(\sigma_1\sqrt{\frac{pq\alpha_2}{\alpha_3}}csch_{pq}(\sqrt{\alpha_2}(x-\omega t))\right)^{1/2}e^{i\theta}. \tag{17}$$

In eqs. (16) and (17) both $\alpha_2,\alpha_3>0$ or $\alpha_2,\alpha_3<0$.

$$u_{1,3}(x,t)=\left(\sigma_1\sqrt{\frac{-pq\alpha_2}{\alpha_3}}sec_{pq}(\sqrt{-\alpha_2}(x-\omega t))\right)^{1/2}e^{i\theta}, \tag{18}$$

$$u_{1,4}(x,t)=\left(\sigma_1\sqrt{\frac{-pq\alpha_2}{\alpha_3}}csc_{pq}(\sqrt{-\alpha_2}(x-\omega t))\right)^{1/2}e^{i\theta}. \tag{19}$$

In eqs. (18) and (19) α_2 and α_3 should have opposite signs. $\theta=\mu x-\lambda t+\psi_0$, sec_{pq}, csc_{pq} and $sech_{pq}$, $csch_{pq}$ are described in Section 2.2 with $p,q>0$.

2.3. Implementation of mNKM to the pGI equation

According to mNKM [63] we propose a new approach for the solution of eq. (6) in the following form:

$$V(\zeta)=\sum_{i=1}^{N}\sigma_0+\sigma_i R(\zeta)^i. \tag{20}$$

If we remember that $N=1$, eq. (20) is converted into:

$$V(\zeta)=\sigma_0+\sigma_1 R(\zeta), \tag{21}$$

where $R(\zeta)$ satisfies the following Riccati ODE;

$$(R'(\zeta))^2=ln^2(A)R^2(\zeta)\left(1-\chi R^2(\zeta)\right),\ 0<A\neq 1. \tag{22}$$

The solution of ODE in eq. (22) are given follows;

$$R(x-\omega t)=\frac{4L}{4L^2A^{(x-\omega t)}+\chi A^{-(x-\omega t)}}, \tag{23}$$

where L,A and χ are non-zero real values to be determined later. Substituting the eq. (21) and eq. (22) into the eq. (6), we obtain a polynomial form of the $R^i(\zeta)$ with $(i=0,1\ldots 8)$. Then by collecting each coefficient of $R(\zeta)$ and equating them to zero, we get the following algebraic system of equations:

$$\begin{aligned}
&\Phi^0(\zeta):-4\sigma_0^2a\mu^2+4b\sigma_0^4-4\mu c\sigma_0^3+4\mu g\sigma_0^3+4\sigma_0^2d\mu+4\sigma_0^2\lambda=0,\\
&\Phi^1(\zeta):2a\sigma_1\sigma_0\ln(A)^2-12\mu c\sigma_0^2\sigma_1+12\mu g\sigma_0^2\sigma_1-8\sigma_0\sigma_1a\mu^2+8\sigma_0\sigma_1d\mu+8\sigma_0\sigma_1\lambda+16b\sigma_0^3\sigma_1=0,\\
&\Phi^2(\zeta):4\sigma_1^2\lambda-12\mu c\sigma_0\sigma_1^2+12\mu g\sigma_0\sigma_1^2+a\sigma_1^2\ln(A)^2+24b\sigma_0^2\sigma_1^2-4a\sigma_1^2\mu^2+4\sigma_1^2d\mu=0,\\
&\Phi^3(\zeta):-4a\sigma_1\sigma_0\ln(A)^2\chi+16b\sigma_0\sigma_1^3-4\mu c\sigma_1^3+4\mu g\sigma_1^3=0,\\
&\Phi^4(\zeta):-3a\sigma_1^2\ln(A)^2\chi+4b\sigma_1^4=0.
\end{aligned} \tag{24}$$

Solving the system in eq. (24), we obtain the following solution set:

$$\mathbf{Set}_2:\left\{b=\frac{3\mu^2(c-g)^2}{16\ln(A)^2a},\ \chi=\frac{\sigma_1^2\mu^2(c-g)^2}{4a^2\ln(A)^4},\ d=\frac{4a\mu^2+5\ln(A)^2a-4\lambda}{4\mu},\ \sigma_0=\frac{2\ln(A)^2a}{\mu(c-g)},\ \sigma_1=\sigma_1\right\}. \tag{25}$$

Substituting eq. (25) into eq. (21) along with eq. (23) and considering $U(\zeta)=\sqrt{V(\zeta)}$, we obtain the following solution:

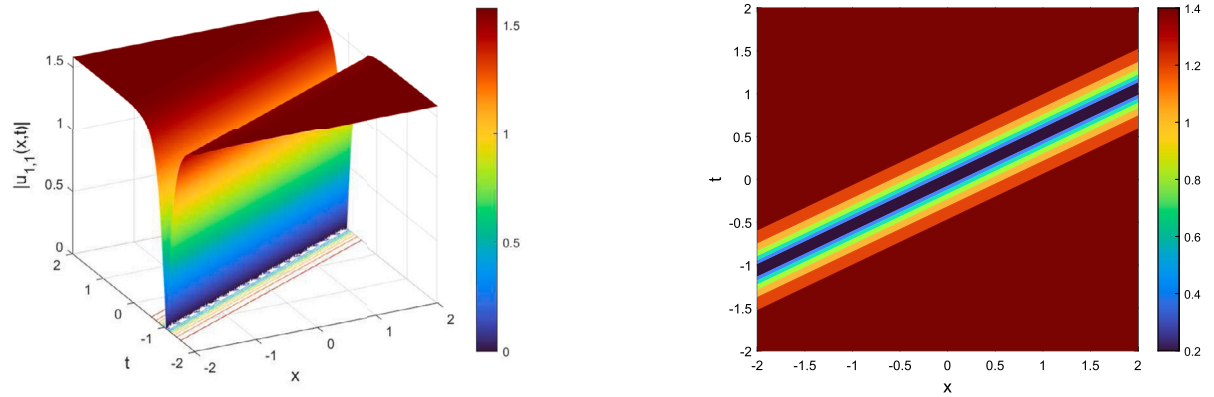
$$u_{2,1}(x,t)=\left(\frac{2\ln(A)^2a}{\mu(c-g)}+\frac{4\sigma_1L}{4L^2A^{(x-\omega t)}+\frac{\sigma_1^2\mu^2(c-g)^2A^{-(x-\omega t)}}{4a^2\ln(A)^4}}\right)^{1/2}e^{i\theta}. \tag{26}$$

3. Results and discussion

This section includes graphical representations of the obtained solution functions and their interpretations.

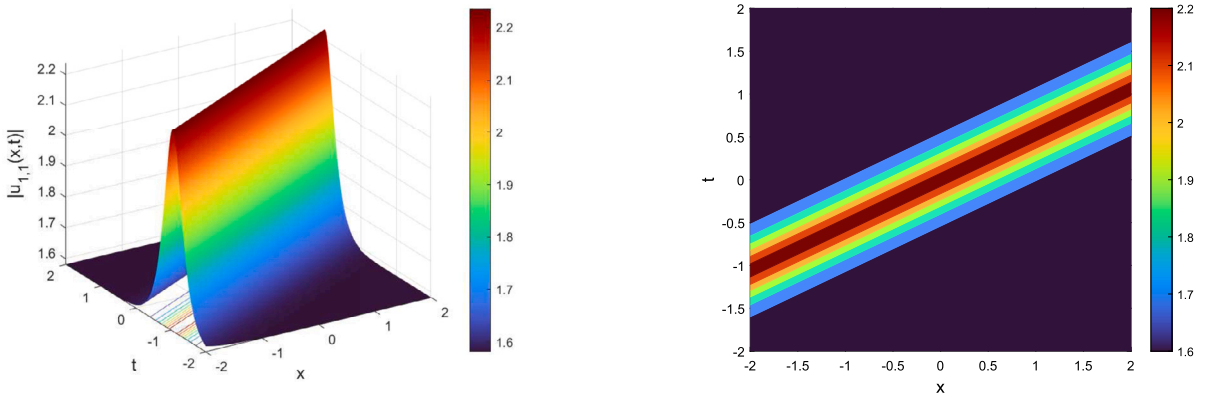
Fig. 1 shows 3D (a) and contour (b) plots of $|u_{1,1}(x,t)|$ in eq. (16) as dark soliton for $\sigma_1=-1,\lambda=1,\mu=4,\psi_0=1,a=0.8,c=-1,\gamma=-2,\alpha_1=0,\alpha_3=-1,p=1$ and $q=1$.

Fig. 2 shows 3D (a) and contour (b) plots of $|u_{1,1}(x,t)|$ in eq. (16) as bright soliton for $\sigma_1=-1,\lambda=1,\mu=4,\psi_0=1,a=0.8,c=-3,\gamma=-2,\alpha_1=0,\alpha_3=-1,p=1$ and $q=1$.



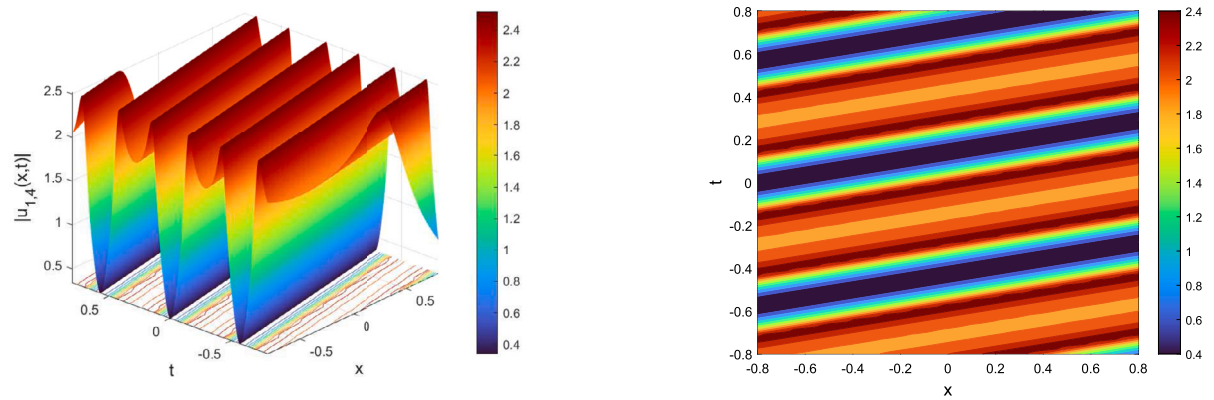
(a) 3D view of $|u_{1,1}(x,t)|$ (b) Contour projection of $|u_{1,1}(x,t)|$

Fig. 1. 3D surface (a), contour plot (b) of modulus $u_{1,1}(x,t)$ in eq. (16).



(a) 3D plot of $|u_{1,1}(x,t)|$ for c=-3 (b) Contour plot of $|u_{1,1}(x,t)|$ for c=-3

Fig. 2. 3D surface (a), contour plot (b) of modulus $u_{1,1}(x,t)$ in eq. (16).

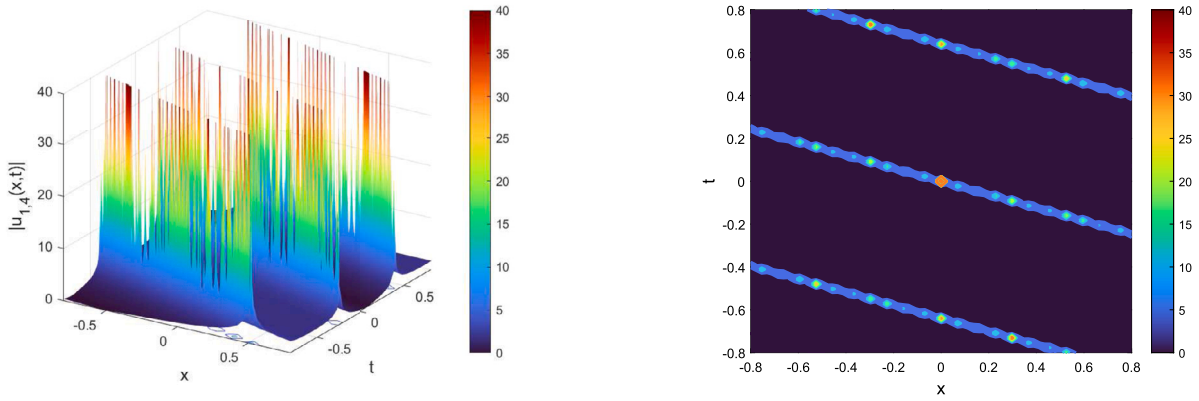


(a) 3D portrait of $|u_{1,4}(x,t)|$ (b) Contour portrait of $|u_{1,4}(x,t)|$

Fig. 3. 3D surface (a), contour plot (b) of modulus $u_{1,4}(x,t)$ in eq. (19).

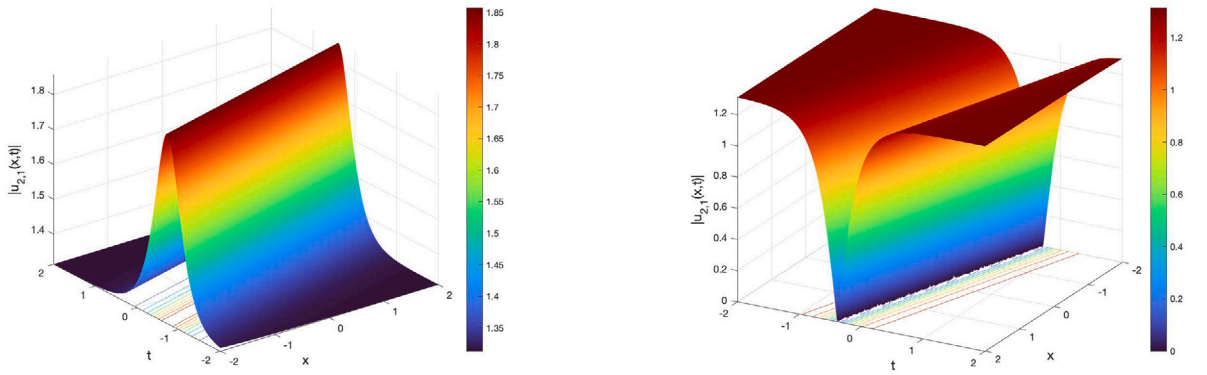
Fig. 3 shows 3D (a) and contour (b) plots of $|u_{1,4}(x,t)|$ in eq. (19) as periodic-M-shaped soliton for $\sigma_1 = -1, \lambda = 1, \mu = 4, \psi_0 = 1, a = 1, c = -1, \gamma = -2, \alpha_1 = 0, \alpha_3 = 1, p = 1$ and $q = 2$.

Fig. 4 shows 3D (a) and contour (b) plots of $|u_{1,4}(x,t)|$ in eq. (19) as periodic-singular soliton for $\sigma_1 = -1, \lambda = 1, \mu = 4, \psi_0 = 1, a = 1, c = -1, \gamma = -2, \alpha_1 = 0, \alpha_3 = 1, p = 1$ and $q = 1$.



(a) 3D simulation of $|u_{2,1}(x,t)|$ (b) Contour simulation of $|u_{2,1}(x,t)|$

Fig. 4. 3D surface (a), contour plot (b) of modulus $u_{1,4}(x,t)$ in eq. (19).



(a) 3D view of $|u_{2,1}(x,t)|$ for μ=-0.7 (b) Contour view of $|u_{2,1}(x,t)|$ for μ=0.7

Fig. 5. 3D surfaces of modulus $u_{2,1}(x,t)$ in eq. (26).

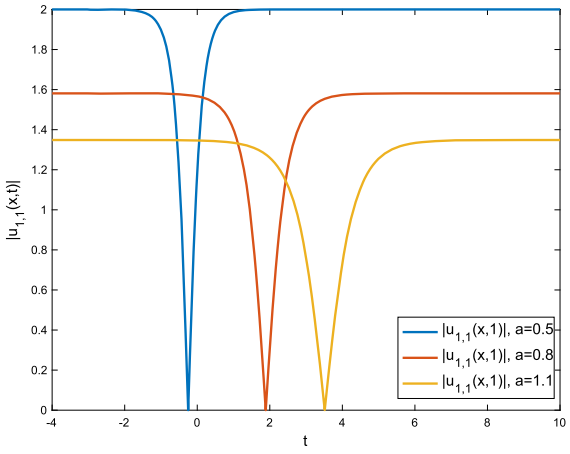
Fig. 5 shows 3D (a,b) plots of $|u_{2,1}(x,t)|$ in eq. (26) as bright and dark soliton for $\sigma_1 = -2, \lambda = -2, \psi_0 = 1, a = 0.5, c = 2, \gamma = 1, A = 3, L = 0.3, \mu = -0.7$ for Fig. 5a and $\mu = 0.7$ for Fig. 5b.

Fig. 6 shows 2D plots of $u_{1,1}(x,t)$ in eq. (16). Figs. 6a and 6b show 2D projections of wave behaviors according to the parameter change. In Fig. 6a, the graphs of the examined soliton are represented by three different colors. Blue, red and yellow-styled waves are plotted with $a = 0.5, 0.8$ and $a = 1.1$ respectively. Parameter a represents the coefficient of the group velocity dispersion term. While parameter a increases, wave amplitude decreases, wavelength increases and the wave shifts through positive x-axis. In Fig. 6b, also depicts the investigated soliton shape by three different colors. Blue, red and yellow-styled waves are plotted for $c = -0.8, -1$ and $c = -1.2$ values. The parameter c represents nonlinear dispersion term. While the parameter c decreases, wave amplitude increases, wavelength decreases and the wave shifts through negative x-axis.

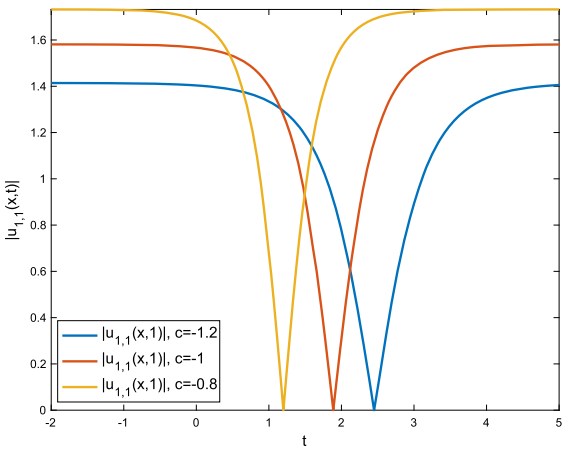
Fig. 7 shows 2D plots of $u_{1,1}(x,t)$ in eq. (16). In Fig. 7a, the wave behavior according to the change of parameter α_3 is depicted. The parameter α_3 is used SSM in eq. (9). There are three-styled waves in Fig. 7a. Blue, red and yellow-styled waves are plotted for $\alpha_3 = -0.8, -1$ and $\alpha_3 = -1.2$ values. While α_3 increases, the wave amplitude decreases and the wave shifts through positive x-axis. In Fig. 7b, we depicted 2D plots to show the change in wave behavior due to change in parameter. In Fig. 7b, there are soliton charts shown with three different colors. Blue, red and yellow-styled waves are plotted for $\gamma = 1.7, 2$ and $\gamma = 2.3$ values, respectively. While the value of γ increases, the wave amplitude increases, the wavelength decreases and the wave shifts through negative x-axis.

Fig. 8 shows 2D plots of $u_{1,1}(x,t)$ in eq. (16). Fig. 8a reflects the wave behavior of the dark soliton depending on the change of μ. Blue, red and yellow-styled waves are plotted for $\mu = 3.2, 4$ and $\mu = 4.8$ values, respectively. While μ increases, the wave amplitude increases, the wavelength decreases and the wave shifts through the positive x-axis. Lastly, Fig. 8b shows wave behavior according to λ. Blue, red and yellow colored lines are plotted for $\lambda = 0.2, 1$ and $\lambda = 1.8$ values, respectively. While λ increases, the wave amplitude and wavelength don't change and the wave shifts through the positive x-axis.

On the basis of the graphic presentations made above and the physical results obtained, let's consider a brief review of their long-term behavior of the obtained solitons:

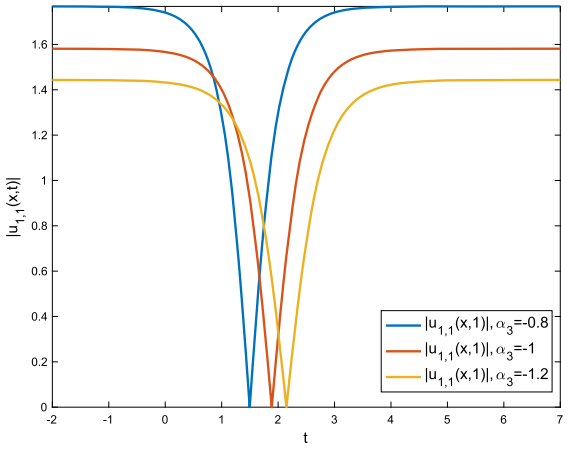


(a) Effect of parameter a on $|u_{1,1}(x,1)|$ in 2D

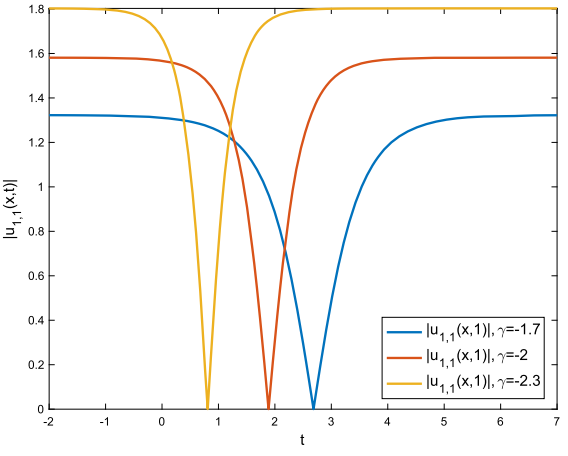


(b) Effect of parameter c on $|u_{1,1}(x,1)|$ in 2D

Fig. 6. 2D plots of modulus of $u_{1,1}(x,t)$ in eq. (16) depending a, c when $t = 1$.

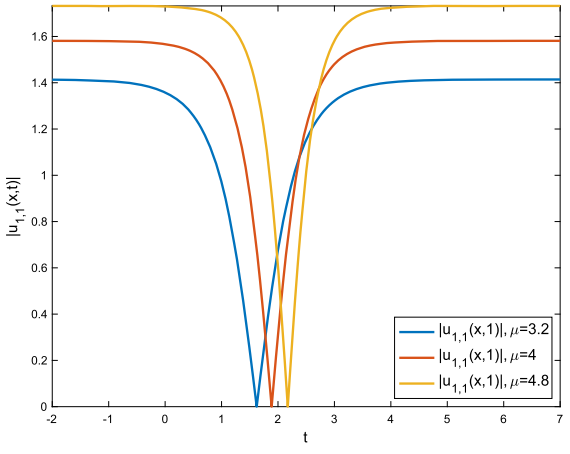


(a) Effect of α_3 on $|u_{1,1}(x,1)|$ in 2D

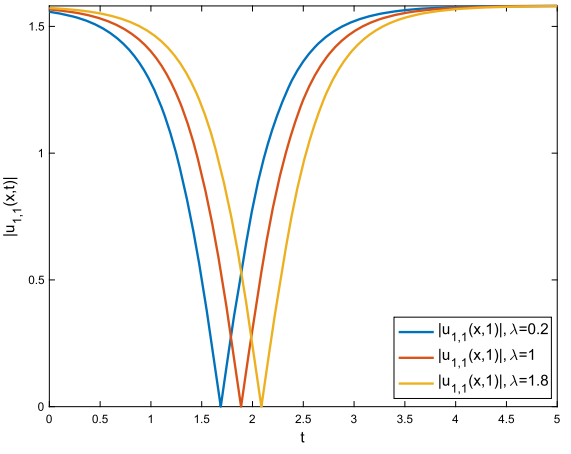


(b) Effect of γ on $|u_{1,1}(x,1)|$ in 2D

Fig. 7. 2D plots of modulus of $u_{1,1}(x,t)$ in eq. (16) depending on α_3, γ when $t = 1$.



(a) Effect of μ on $|u_{1,1}(x,1)|$ in 2D



(b) Effect of λ on $|u_{1,1}(x,1)|$ in 2D

Fig. 8. 2D plots of modulus of $u_{1,1}(x,t)$ in eq. (16) depending on μ, λ when $t = 1$.

Let consider $u_{1,1}(x,t), u_{1,2}(x,t), u_{1,3}(x,t), u_{1,4}(x,t)$ solutions which were given in eqs. (16) to (19) and consider the figures of these solutions which were depicted in Figs. 1 to 4. In Fig. 1, $|u_{1,1}(x,t)| = k \in \mathbf{R}$ for $t \mapsto \pm\infty$ and similarly $|u_{1,1}(x,t)| = k \in \mathbf{R}$ for $x \mapsto \pm\infty$ (k is the amplitude of the dark soliton). In Fig. 2, $|u_{1,1}(x,t)| = 0$ for $t \mapsto \pm\infty$ and similarly $|u_{1,1}(x,t)| = 0$ for $x \mapsto \pm\infty$. In Fig. 3, it is seen that the soliton behavior is in the form of a sinusoidal occurring with different amplitudes when $t \mapsto \pm\infty$ and $x \mapsto \pm\infty$. In Fig. 4, singular soliton behavior occurring with soliton amplitude as $\lim_{t \mapsto t_0} |u_{1,4}(x,t)| \mapsto \infty, \lim_{x \mapsto x_0} |u_{1,4}(x,t)| \mapsto \infty$ at some values for $t \mapsto t_0$ and $x \mapsto x_0$. These investigated solutions belong to the SSM. Also, we can analyze the solution obtained via mNKM. Let consider the Fig. 5 and eq. (26) together, $\lim_{t \mapsto \pm\infty} |u_{2,1}(x,t)| = 0$ and $\lim_{x \mapsto \pm\infty} |u_{2,1}(x,t)| = 0$ in Fig. 5a. $\lim_{t \mapsto \pm\infty} |u_{2,1}(x,t)| = M \in R$ and $\lim_{x \mapsto \pm\infty} |u_{2,1}(x,t)| = M \in R$ in which M represents the amplitude of the dark soliton which is generated by different parameters in Fig. 5b.

4. Conclusion

In our study, we have used two effective analytical methods, the Sardar sub-equation and the modified new Kudryashov method, to obtain new soliton solutions of the perturbed Gerdjikov-Ivanov equation, which is a Schrödinger-based model used in fiber optic communication. Our main motivation in this study is that the soliton solutions of the pGI equation have never been analyzed before with these two methods. As a result of the application, dark, bright, periodic-singular, periodic-M-shaped soliton solutions have been obtained. It should also be noted that periodic-M-shaped solitons are very rare in the solutions set. We have obtained periodic-M-shaped soliton in eq. (19) and 3D and contour graphics of compacton soliton have been placed in Fig. 3. In addition, the 3D, 2D and contour graphics of the obtained soliton solutions have been drawn using Symbolic Algebra Software (Matlab R2022a), and the effects of the parameters in the model and method have been examined and interpreted with 2D graphics. According to the findings we have reached at the end of the study, it is highly probable that the soliton solutions obtained will give an idea to many researchers working in the field of fiber optics, while emphasizing that the proposed methods are not complicated, give fast results, are effective, reliable and widely used by many researchers in different models.

Author contribution statement

Mustafa Bayram: Conceived and designed the experiments; Wrote the paper. Aydin Secer: Performed the experiments. Ismail Onder: Analyzed and interpreted the data. Muslum Ozisik: Contributed reagents, materials, analysis tools or data.

Funding statement

This research did not receive any specific grant from funding agencies in the public, commercial, or not-for-profit sectors.

Declaration of competing interest

The authors declare no competing interests.

Data availability

No data was used for the research described in the article.

References

[1] G.C. Calafiore, C. Novara, C. Possieri, A modified sir model for the Covid-19 contagion in Italy, in: Proceedings of the IEEE Conference on Decision and Control 2020-December, 2020, pp. 3889–3894.
[2] L. Ingber, Statistical-mechanical aids to calculating term-structure models, Phys. Rev. A 42 (1990) 7057, https://doi.org/10.1103/PhysRevA.42.7057.
[3] A.R. Kasimov, L.M. Faria, R.R. Rosales, Model for shock wave chaos, Phys. Rev. Lett. 110 (2013) 104104, https://doi.org/10.1103/PHYSREVLETT.110.104104.
[4] M. Cinar, I. Onder, A. Secer, M. Bayram, A. Yusuf, T.A. Sulaiman, A comparison of analytical solutions of nonlinear complex generalized zakharov dynamical system for various definitions of the differential operator, Electron. Res. Arch. 1 (30) (2022) 335–361, https://doi.org/10.3934/ERA.2022018.
[5] B.E. Lo, C.C. Mei, A numerical study of water-wave modulation based on a higher-order nonlinear Schrodinger equation, J. Fluid Mech. 150 (1985) 395–416, https://doi.org/10.1017/S0022112085000180.
[6] K.L. Henderson, D.H. Peregrine, J.W. Dold, Unsteady water wave modulations: fully nonlinear solutions and comparison with the nonlinear Schrödinger equation, Wave Motion 29 (4) (1999) 341–361, https://doi.org/10.1016/s0165-2125(98)00045-6.
[7] K. Dysthe, Note on a modification to the nonlinear Schrödinger equation for application to deep water waves, Proc. R. Soc. Lond. Ser. A, Math. Phys. Sci. 369 (1736) (1979) 105–114, https://doi.org/10.1098/rspa.1979.0154.
[8] C.C. Ding, Y.T. Gao, G.F. Deng, D. Wang, Lax pair, conservation laws, Darboux transformation, breathers and rogue waves for the coupled nonautonomous nonlinear Schrödinger system in an inhomogeneous plasma, Chaos Solitons Fractals 133 (2020) 109580, https://doi.org/10.1016/j.chaos.2019.109580.
[9] J.H. Lee, O.K. Pashaev, C. Rogers, W.K. Schief, The resonant nonlinear Schrödinger equation in cold plasma physics. Application of Bäcklund-Darboux transformations and superposition principles, J. Plasma Phys. 73 (2) (2007) 257–272, https://doi.org/10.1017/S0022377806004648.
[10] J. Hermann, Z. Schätzle, F. Noé, Deep-neural-network solution of the electronic Schrödinger equation, Nat. Chem. 12 (10) (2020) 891–897, https://doi.org/10.1038/s41557-020-0544-y, arXiv:1909.08423.
[11] R. Bekenstein, R. Schley, M. Mutzafi, C. Rotschild, M. Segev, Optical simulations of gravitational effects in the Newton-Schrödinger system, Nat. Phys. 11 (10) (2015) 872–878, https://doi.org/10.1038/nphys3451.
[12] K. Hosseini, M. Mirzazadeh, D. Baleanu, S. Salahshour, L. Akinyemi, Optical solitons of a high-order nonlinear Schrödinger equation involving nonlinear dispersions and Kerr effect, Opt. Quantum Electron. 54 (3) (2022) 1–12, https://doi.org/10.1007/s11082-022-03522-0.

[13] D. Cai, A.R. Bishop, N. Grønbech-Jensen, B.A. Malomed, Dark shock waves in the nonlinear schrödinger system with internal losses, Phys. Rev. Lett. 78 (2) (1997) 223–226, https://doi.org/10.1103/PhysRevLett.78.223.
[14] R. Chteoui, A.F. Aljohani, A.B. Mabrouk, Classification and simulation of chaotic behavior of the solutions of a mixed nonlinear Schrodinger system, Electron. Res. Arch. 29 (4) (2021) 2561–2597, https://doi.org/10.3934/era.2021002.
[15] A. Navarrete, A. Paredes, J.R. Salgueiro, H. Michinel, Spatial solitons in thermo-optical media from the nonlinear Schrödinger-Poisson equation and dark-matter analogs, Phys. Rev. A 95 (1) (2017) 013844, https://doi.org/10.1103/PhysRevA.95.013844, arXiv:1703.09095.
[16] M.J. Potasek, An analysis of the coefficients of a perturbed nonlinear Schrödinger equation for femtosecond behavior in an optical waveguide, J. Appl. Phys. 63 (10) (1988) 5186–5188, https://doi.org/10.1063/1.340378.
[17] N. Raza, S. Arshed, A. Javid, Optical solitons and stability analysis for the generalized second-order nonlinear Schrödinger equation in an optical fiber, Int. J. Nonlinear Sci. Numer. Simul. 21 (7) (2020) 855–863, https://doi.org/10.1515/ijnsns-2019-0287.
[18] K. Hosseini, E. Hincal, S. Salahshour, M. Mirzazadeh, K. Dehigia, B. Nath, On the dynamics of soliton waves in a generalized nonlinear Schrödinger equation, Optik 272 (2022) 170215, https://doi.org/10.1016/j.ijleo.2022.170215.
[19] A.H. Arnous, Q. Zhou, A. Biswas, P. Guggilla, S. Khan, Y. Yıldırım, A.S. Alshomrani, H.M. Alshehri, Optical solitons in fiber Bragg gratings with cubic–quartic dispersive reflectivity by enhanced Kudryashov's approach, Phys. Lett. Sect. A, Gen. At. Solid State Phys. 422 (2022) 127797, https://doi.org/10.1016/j.physleta.2021.127797.
[20] A.H. Arnous, M.Z. Ullah, M. Asma, S.P. Moshokoa, M. Mirzazadeh, A. Biswas, M. Belic, Nematicons in liquid crystals by modified simple equation method, Nonlinear Dyn. 88 (4) (2017) 2863–2872, https://doi.org/10.1007/s11071-017-3416-2.
[21] J. Vega-Guzman, M.F. Mahmood, Q. Zhou, H. Triki, A.H. Arnous, A. Biswas, S.P. Moshokoa, M. Belic, Solitons in nonlinear directional couplers with optical metamaterials, Nonlinear Dyn. 87 (1) (2017) 427–458, https://doi.org/10.1007/s11071-016-3052-2.
[22] H. Triki, A. Biswas, Dark solitons for a generalized nonlinear Schrödinger equation with parabolic law and dual-power law nonlinearities, Math. Methods Appl. Sci. 34 (8) (2011) 958–962, https://doi.org/10.1002/mma.1414.
[23] A. Biswas, D. Milovic, Bright and dark solitons of the generalized nonlinear Schrödinger's equation, Commun. Nonlinear Sci. Numer. Simul. 15 (6) (2010) 1473–1484, https://doi.org/10.1016/j.cnsns.2009.06.017.
[24] H. Esen, N. Ozdemir, A. Secer, M. Bayram, On solitary wave solutions for the perturbed Chen–Lee–Liu equation via an analytical approach, Optik 245 (2021) 167641, https://doi.org/10.1016/j.ijleo.2021.167641.
[25] A.H. Arnous, M. Mirzazadeh, A. Akbulut, L. Akinyemi, Optical solutions and conservation laws of the Chen–Lee–Liu equation with Kudryashov's refractive index via two integrable techniques, in: Waves in Random and Complex Media, 2022.
[26] H. Esen, N. Ozdemir, A. Secer, M. Bayram, T.A. Sulaiman, A. Yusuf, Solitary wave solutions of chiral nonlinear Schrödinger equations, Mod. Phys. Lett. B 35 (30) (sep 2021), https://doi.org/10.1142/S0217984921504728.
[27] S. Saha Ray, Dispersive optical solitons of time-fractional Schrödinger–Hirota equation in nonlinear optical fibers, Phys. A, Stat. Mech. Appl. 537 (2020) 122619, https://doi.org/10.1016/j.physa.2019.122619.
[28] M. El-Borai, H. El-Owaidy, H.M. Ahmed, A.H. Arnous, S. Moshokoa, A. Biswas, M. Belic, Topological and singular soliton solution to Kundu–Eckhaus equation with extended Kudryashov's method, Optik 128 (2017) 57–62, https://doi.org/10.1016/j.ijleo.2016.10.011.
[29] A.H. Arnous, M. Mirzazadeh, Application of the generalized Kudryashov method to the Eckhaus equation, Nonlinear Anal., Model. Control 21 (5) (2016) 577–586, https://doi.org/10.15388/NA.2016.5.1.
[30] K. Hosseini, M. Mirzazadeh, J.F. Gómez-Aguilar, Soliton solutions of the Sasa–Satsuma equation in the monomode optical fibers including the beta-derivatives, Optik 224 (2020) 165425, https://doi.org/10.1016/j.ijleo.2020.165425.
[31] M. Ozisik, On the optical soliton solution of the (1 + 1)-dimensional perturbed NLSE in optical nano-fibers, Optik 250 (2022) 168233, https://doi.org/10.1016/J.IJLEO.2021.168233.
[32] M. Cinar, I. Onder, A. Secer, T.A. Sulaiman, A. Yusuf, M. Bayram, Optical solitons of the (2 + 1)-dimensional Biswas–Milovic equation using modified extended tanh-function method, Optik 245 (2021) 167631, https://doi.org/10.1016/j.ijleo.2021.167631.
[33] A.H. Arnous, Optical solitons with Biswas–Milovic equation in magneto-optic waveguide having Kudryashov's law of refractive index, Optik 247 (2021) 167987, https://doi.org/10.1016/j.ijleo.2021.167987.
[34] K. Hosseini, M. Mirzazadeh, L. Akinyemi, D. Baleanu, S. Salahshour, Optical solitons to the Ginzburg–Landau equation including the parabolic nonlinearity, Opt. Quantum Electron. 54 (10) (2022), https://doi.org/10.1007/s11082-022-03884-5.
[35] A.H. Arnous, A. Biswas, Y. Yıldırım, Q. Zhou, W. Liu, A.S. Alshomrani, H.M. Alshehri, Cubic–quartic optical soliton perturbation with complex Ginzburg–Landau equation by the enhanced Kudryashov's method, Chaos Solitons Fractals 155 (2022) 111748, https://doi.org/10.1016/j.chaos.2021.111748.
[36] A.H. Arnous, L. Moraru, Optical solitons with the complex Ginzburg–Landau equation with Kudryashov's law of refractive index, Mathematics 10 (19) (2022) 3456, https://doi.org/10.3390/math10193456.
[37] A. Biswas, J. Vega-Guzman, A. Bansal, A.H. Kara, A.K. Alzahrani, Q. Zhou, M.R. Belic, Optical dromions, domain walls and conservation laws with Kundu–Mukherjee–Naskar equation via traveling waves and Lie symmetry, Results Phys. 16 (2020) 102850, https://doi.org/10.1016/j.rinp.2019.102850.
[38] A.S.K.A. Selvakumaran, S.D. Purohit, M. Bayram, Convexity of certain -integral operators of valent functions, Abstr. Appl. Anal. 2014 (2014) 2014, https://doi.org/10.1155/2014/925902.
[39] K. Hosseini, M. Inc, M. Shafiee, M. Ilie, A. Shafaroody, A. Yusuf, M. Bayram, Invariant subspaces, exact solutions and stability analysis of nonlinear water wave equations, J. Ocean Eng. Sci. 5 (1) (2020) 35–40, https://doi.org/10.1016/j.joes.2019.07.004.
[40] A. Yusuf, T.A. Sulaiman, E. Khalil, M. Bayram, H. Ahmad, Construction of multi-wave complexiton solutions of the kadomtsev-petviashvili equation via two efficient analyzing techniques, Results Phys. 21 (2021) 103775, https://doi.org/10.1016/j.rinp.2020.103775.
[41] M. Bayram, Automatic analysis of the control of metabolic networks, Comput. Biol. Med. 26 (5) (1996) 401–408, https://doi.org/10.1016/0010-4825(96)00011-X.
[42] B. Ibis, M. Bayram, Approximate solutions for some nonlinear evolutions equations by using the reduced differential transform method, Int. J. Appl. Math. Res. 1 (3) (2012) 288–302.
[43] A. Biswas, R.T. Alqahtani, Chirp-free bright optical solitons for perturbed Gerdjikov–Ivanov equation by semi-inverse variational principle, Optik 147 (2017) 72–76, https://doi.org/10.1016/j.ijleo.2017.08.019.
[44] A. Biswas, Y. Yildirim, E. Yasar, H. Triki, A.S. Alshomrani, M.Z. Ullah, Q. Zhou, S.P. Moshokoa, M. Belic, Optical soliton perturbation with Gerdjikov–Ivanov equation by modified simple equation method, Optik 157 (2018) 1235–1240, https://doi.org/10.1016/j.ijleo.2017.12.101.
[45] K.K. Al-Kalbani, K.S. Al-Ghafri, E.V. Krishnan, A. Biswas, Solitons and modulation instability of the perturbed Gerdjikov–Ivanov equation with spatio-temporal dispersion, Chaos Solitons Fractals 153 (2021) 111523, https://doi.org/10.1016/j.chaos.2021.111523.
[46] A. Biswas, Y. Yildirim, E. Yasar, H. Triki, A.S. Alshomrani, M.Z. Ullah, Q. Zhou, S.P. Moshokoa, M. Belic, Optical soliton perturbation with full nonlinearity for Gerdjikov–Ivanov equation by trial equation method, Optik 157 (2018) 1214–1218, https://doi.org/10.1016/j.ijleo.2017.12.099.
[47] S. Arshed, Two reliable techniques for the soliton solutions of perturbed Gerdjikov–Ivanov equation, Optik 164 (2018) 93–99, https://doi.org/10.1016/j.ijleo.2018.02.119.
[48] A. Biswas, Y. Yıldırım, E. Yaşar, Q. Zhou, A.S. Alshomrani, S.P. Moshokoa, M. Belic, Solitons for perturbed Gerdjikov–Ivanov equation in optical fibers and PCF by extended Kudryashov's method, Opt. Quantum Electron. 50 (3) (2018) 1–13, https://doi.org/10.1007/s11082-018-1417-0.
[49] M.S. Ahmed, A.S. Zaghrout, H.M. Ahmed, A.H. Arnous, Optical soliton perturbation of the Gerdjikov–Ivanov equation with spatio-temporal dispersion using a modified extended direct algebraic method, Optik 259 (2022) 168904, https://doi.org/10.1016/j.ijleo.2022.168904.

[50] A. Muniyappan, P. Monisha, E.K. Priya, V. Nivetha, Generation of wing-shaped dark soliton for perturbed Gerdjikov–Ivanov equation in optical fibre, Optik 230 (2021) 166328, https://doi.org/10.1016/j.ijleo.2021.166328.
[51] M.S. Osman, A. Zafar, K.K. Ali, W. Razzaq, Novel optical solitons to the perturbed Gerdjikov–Ivanov equation with truncated M-fractional conformable derivative, Optik 222 (2020) 103825, https://doi.org/10.1016/j.ijleo.2020.165418.
[52] E. Yaşar, Y. Yıldırım, E. Yaşar, New optical solitons of space-time conformable fractional perturbed Gerdjikov-Ivanov equation by sine-Gordon equation method, Results Phys. 9 (2018) 1666–1672, https://doi.org/10.1016/j.rinp.2018.04.058.
[53] C. Li, G. Li, L. Chen, Fractional optical solitons of the space-time perturbed fractional Gerdjikov-Ivanov equation, Optik 224 (2020) 165638, https://doi.org/10.1016/j.ijleo.2020.165638.
[54] A. Biswas, Y. Yıldırım, E. Yaşar, M.M. Babatin, Conservation laws for Gerdjikov-Ivanov equation in nonlinear fiber optics and PCF, Optik 148 (2017) 209–214, https://doi.org/10.1016/j.ijleo.2017.08.094.
[55] M.M. Khater, Abundant wave solutions of the perturbed Gerdjikov-Ivanov equation in telecommunication industry, Mod. Phys. Lett. B 35 (26) (aug 2021), https://doi.org/10.1142/S021798492150456X.
[56] H. Li, New solitary wave solutions for the perturbed Gerdjikov-Ivanov equation, in: Authorea Preprints, mar 2022.
[57] Z. Li, T. Han, Classification of all single traveling wave solutions of fractional perturbed Gerdjikov-Ivanov equation, Math. Probl. Eng. 2021 (2021), https://doi.org/10.1155/2021/1283083.
[58] Z. Hassan, N. Raza, J.F. Gómez-Aguilar, Novel optical solitons to the perturbed Gerdjikov–Ivanov equation via collective variables, Opt. Quantum Electron. 53 (8) (2021) 1–19, https://doi.org/10.1007/s11082-021-03123-3.
[59] I. Samir, N. Badra, A.R. Seadawy, H.M. Ahmed, A.H. Arnous, Computational extracting solutions for the perturbed Gerdjikov-Ivanov equation by using improved modified extended analytical approach, J. Geom. Phys. 176 (2022) 104514, https://doi.org/10.1016/j.geomphys.2022.104514.
[60] H. Rezazadeh, M. Inc, D. Baleanu, New solitary wave solutions for variants of (3+1)-dimensional Wazwaz-Benjamin-Bona-Mahony equations, Front. Phys. 8 (2020) 332, https://doi.org/10.3389/fphy.2020.00332.
[61] E.M. Zayed, M.E. Alngar, A. Biswas, M. Asma, M. Ekici, A.K. Alzahrani, M.R. Belic, Optical solitons and conservation laws with generalized kudryashov's law of refractive index, Chaos Solitons Fractals 139 (2020) 110284, https://doi.org/10.1016/J.CHAOS.2020.110284.
[62] H. Alotaibi, Traveling wave solutions to the nonlinear evolution equation using expansion method and addendum to kudryashov's method, Symmetry 13 (2021) 2126, https://doi.org/10.3390/SYM13112126.
[63] M. Ozisik, A. Secer, M. Bayram, H. Aydin, An encyclopedia of Kudryashov's integrability approaches applicable to optoelectronic devices, Optik 265 (2022) 169499, https://doi.org/10.1016/j.ijleo.2022.169499.